Lunar influence on equatorial atmospheric angular momentum

Christian Bizouard, Leonid Zotov, Nikolay Sidorenkov

AGU PUBLICATIONS

JGR

Journal of Geophysical Research: Atmospheres

RESEARCH ARTICLE

10.1002/2014JD022240

Key Points:
- Equatorial atmospheric angular momentum studied in the nonrotating frame
- Two main peaks: harmonic at 13.6 days (O_1) and broadband peak around 7 days
- The 13.6 day cycle is explained by an equilibrium lunar tide model

Correspondence to:
C. Bizouard,
christian.bizouard@obspm.fr

Citation:
Bizouard, C., L. Zotov, and N. Sidorenkov (2014), Lunar influence on equatorial atmospheric angular momentum, *J. Geophys. Res. Atmos.*, *119*, 11,920–11,931, doi:10.1002/2014JD022240.

Received 28 JUN 2014
Accepted 2 OCT 2014
Accepted article online 8 OCT 2014
Published online 7 NOV 2014

Lunar influence on equatorial atmospheric angular momentum

Christian Bizouard[1], Leonid Zotov[2], and Nikolay Sidorenkov[3]

[1]Paris Observatory SYRTE, CNRS/UMR 8630, UPMC, [2]Sternberg Astronomical Institute, Moscow State University, Moscow, Russia, [3]Hydrometeorological Centre/Global Atmospheric Circulation Laboratory of Russia, Moscow, Russia

Abstract This study investigates the relationship between the equatorial atmospheric angular momentum oscillation in the nonrotating frame and the quasi-diurnal lunar tidal potential. Between 2 and 30 days, the corresponding equatorial component, called Celestial Atmospheric Angular Momentum (CEAM), is mostly constituted of prograde circular motions, especially of a harmonic at 13.66 days, a sidelobe at 13.63 days, and of a weekly broadband variation. A simple equilibrium tide model explains the 13.66 day pressure term as a result of the O_1 lunar tide. The powerful episodic fluctuations between 5 and 8 days possibly reflect an atmospheric normal mode excited by the tidal waves Q_1 (6.86 days) and σ_1 (7.095 days). The lunar tidal influence on the spectral band from 2 to 30 days is confirmed by two specific features, not occurring for seasonal band dominated by the solar thermal effect. First, Northern and Southern Hemispheres contribute equally and synchronously to the CEAM wind term. Second, the pressure and wind terms are proportional, which follows from angular momentum budget considerations where the topographic and friction torques on the solid Earth are much smaller than the one resulting from the equatorial bulge. Such a configuration is expected for the case of tidally induced circulation, where the surface pressure variation is tesseral and cannot contribute to the topographic torque, and tidal winds blow only at high altitudes. The likely effects of the lunar-driven atmospheric circulation on Earth's nutation are estimated and discussed in light of the present-day capabilities of space geodetic techniques.

1. Introduction

According to investigations going back to the nineteenth century (encapsulated in *Chapman and Lindzen* [1970]) and more recent ones like *Sidorenkov* [2009, 2010a, 2010b], the lunar tide influences the atmospheric circulation. Its effect has been detected in wind and pressure fields as well as in the globally integrated atmospheric angular momentum. Given the angular momentum exchange between the solid Earth and the atmosphere, the atmospheric lunar tide also couples to Earth rotation variations, namely, to length of day [*Li*, 2005; *Li et al.*, 2011], possibly to fortnightly polar motion [*Bizouard and Seoane*, 2010], and to the 13.6 day nutation [*Brzeziński et al.*, 2002; *Sidorenkov*, 2009].

Besides prominent quasi-biennial, seasonal, and rapid oscillations, the Equatorial Atmospheric Angular Momentum (EAAM) exhibits retrograde quasi-diurnal variations of comparable magnitude. Its main peaks at 24 h (S_1), 24.07 h (P_1), and 23.93 h (K_1) are commonly interpreted as the effect of diurnal solar thermal heating (24 h) subject to a yearly amplitude modulation [*Zharov*, 1997; *Bizouard et al.*, 1998]. Squeezed in a frequency band around 24 h in the Terrestrial Reference Frame (TRF), the corresponding periodicities stretch from 2 days to several years with respect to the nonrotating reference frame. This interdependence follows from the fundamental relationship that—with $\Omega = 2\pi$ 1.002738 rad/d being Earth's mean stellar angular frequency—any diurnal component of frequency $\sigma = -\Omega + \sigma'$ with $\sigma' \ll \Omega$ is mapped to a long periodic celestial component of frequency σ'. Removal of the diurnal carrier in the TRF-based EAAM therefore produces Celestial Atmospheric Angular Momentum (CEAM) [*Brzeziński*, 1994] that represents retrograde diurnal oscillations as slow periodic variations. Such "demodulated" time series form the basis for a characterization of the effects of the major retrograde diurnal components (S_1, P_1, and K_1) on Earth's precession nutation [*Bizouard et al.*, 1998; *Yseboodt et al.*, 2002; *Brzeziński et al.*, 2002].

Some of the cited studies mention the existence of a minor but sharp 25.82 h peak [*Brzeziński et al.*, 2002] and evasively attribute it to the O_1 lunar tesseral tide, considering the absence of thermal processes at this frequency. It has been also noticed that in the nonrotating equatorial frame, this equatorial oscillation has a period of $1/(24/25.82 - 1.00273) = 13.6$ days and thus excites the well-known 13.6 day nutation. The present paper attempts to deepen the insight into this signal component by a detailed analysis of CEAM

variations from 2 to 30 days in the nonrotating frame. Specifically, the coherence of the 13.6 day harmonic with the lunar gravitational tide will be shown.

2. Basic Relationships and Celestial Atmospheric Angular Momentum

Let H_i be the Cartesian components of the Atmospheric Angular Momentum (AAM) vector in the TRF, $C = 8.0370\,10^{37}$ kg m^2 the mean axial moment of inertia, and $A = 8.0101\,10^{37}$ kg m^2 the mean equatorial moment of inertia. At subsecular time scales, Earth rotation variations are commonly investigated by the linear Liouville equations, where the excitation of any surface fluid layer maps into a nondimensional terrestrial quantity χ_i of the angular momentum of this layer:

$$\chi_1 = \frac{H_1}{(C-A)\Omega}\,,\ \chi_2 = \frac{H_2}{(C-A)\Omega}\,,\ \chi_3 = \frac{H_3}{C\Omega}\,. \tag{1}$$

The χ_i are called Angular Momentum Functions (AMF) and are composed of two terms: (i) the first, produced by the rotation of the air mass distribution, can be computed from surface pressure data and is usually called *pressure term* and (ii) the second, caused by the winds, is proportional to the relative angular momentum of the atmosphere and might be denoted as *wind term* [*Barnes et al.*, 1983]. Note that in order to account for Earth's nonrigidity in the Liouville equations, the AMF have to be multiplied by appropriate coefficients close to 1, yielding the so-called Effective Angular Momentum Function (EAMF) [*Barnes et al.*, 1983].

The components $\underline{\chi''}$ in the true equatorial frame *GXYZ*—characterized by a fundamental plane perpendicular to the Celestial Intermediate Pole and the Conventional Intermediate Origin [*IERS Conventions*, 2010]—can be derived from their terrestrial counterparts $\underline{\chi}$ by applying the matrix transformation

$$\underline{\chi''} = R_3 W \underline{\chi}\,, \tag{2}$$

where R_3 represents the diurnal rotation and W the polar motion. The major part of this transformation is caused by the uniform rotation in R_3 with the mean angular velocity Ω. We argue that the residual rotation can be considered as a perturbation. At subsecular time scales, polar motion produces oscillations of the geographic pole below 1 arc sec, and the nonuniform part of the rotation angle in R_3 is smaller than 20 arc sec. As the χ_i are small quantities of the order of 10^{-7} rad, the maximum effect of the variable rotation is $20 \times 10^{-7} = 2\,10^{-6}$ arc sec over 100 years, which can be neglected in light of the AAM accuracy ($> 10^{-4}$ arc sec). Thus, for subsecular phenomena, the above transformation can be restricted to an axial rotation reading

$$\underline{\chi''} = R_3[\theta(t)]\underline{\chi}\,, \tag{3}$$

where $\theta(t)$ is the uniformly varying rotation angle

$$\theta(t) = \theta(\mathrm{TAI}_0) + \Omega(\mathrm{TAI} - \mathrm{TAI}_0)\,, \tag{4}$$

with TAI_0 being a conventionally chosen instant of TAI (Temps Atomique International). Taking TAI_0 as 1 January 2000 at UT 1 noon and following *IERS Conventions* [2010, chapter 5, equation (5.14)], the angle $\theta(\mathrm{TAI}_0)$ of this reference date is $\theta(\mathrm{TAI}_0) = 2\pi\,0.779\,057\,273\,2640 \approx -79.53°$.

The rotation in (3) leaves the axial component unchanged ($\chi_3'' = \chi_3$), while the complex equatorial quantity $\chi = \chi_1 + i\chi_2$ is converted to

$$\chi'' = \chi e^{i\theta(t)}\,. \tag{5}$$

To estimate the nutation influence produced by a fluid layer excitation, *Brzeziński* [1994] derived the Liouville equation in the nonrotating equatorial system *GXYZ* and introduced the quantity CEAM function defined by

$$\chi' = -\chi e^{i\,\mathrm{GST}} \approx -\chi e^{i\,\theta(t)} = -\chi''\,, \tag{6}$$

where GST signifies the Greenwich Sidereal Time. In order to comply with the recommendations issued by the International Earth Rotation and Reference System Service (IERS) for parameterizing Earth's rotation, GST is replaced by the Earth rotation angle θ [*IERS Conventions*, 2010], and hence, the CEAM function is defined by

$$\chi' = -\chi e^{i\theta(t)}\,. \tag{7}$$

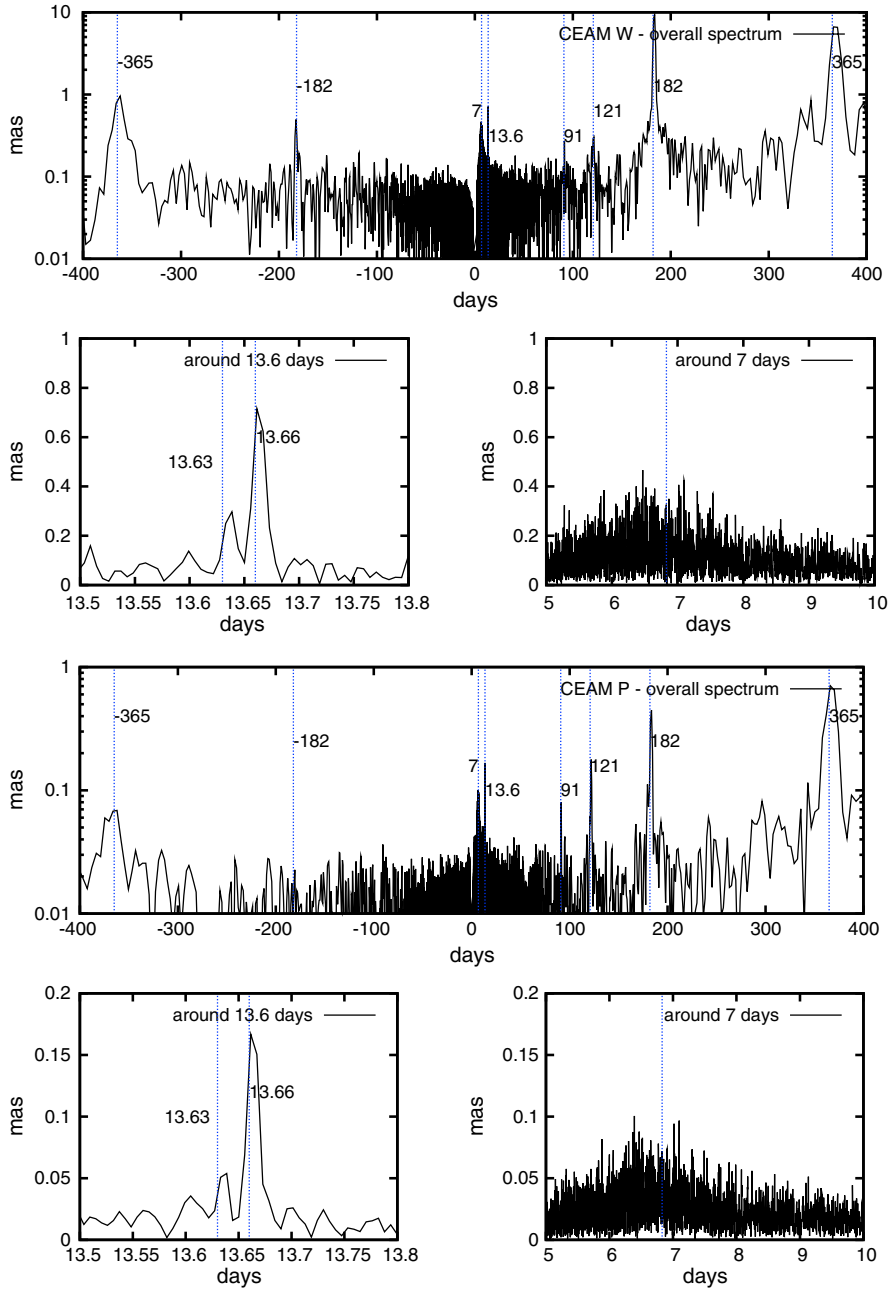

Figure 1. Amplitude spectrum of the Celestial Angular Momentum, (top) Wind (W) and (bottom) Pressure (P) components over the period 1949–2012. Data source: NCEP/NCAR.

3. Analysis of the CEAM

Using 6-hourly EAMF estimates from the reanalysis model of NCEP/NCAR (National Center for Environmental Prediction/National Center of Atmospheric Research) over the period 1949–2013, as provided by the Global Geophysical Fluids Center of the IERS [*SBA*, 2014], we computed the associated CEAM according to (7) for both pressure and wind terms. Prior to demodulation, we removed the long-term components (periods larger than 2 days) of the AAM. After application of (7), a low-band-pass filter was used to eliminate residual diurnal/subdiurnal signal content and to obtain the celestial excitation limited to periods larger than 2 days, corresponding to the precession-nutation frequency band.

The complex Fourier spectrum of the obtained CEAM is displayed in Figure 1. It is dominated by a prograde annual oscillation at 365 days (S_1 in the TRF) and its subharmonics at 182 (P_1), 121 (π_1), and 91 days (1.0083

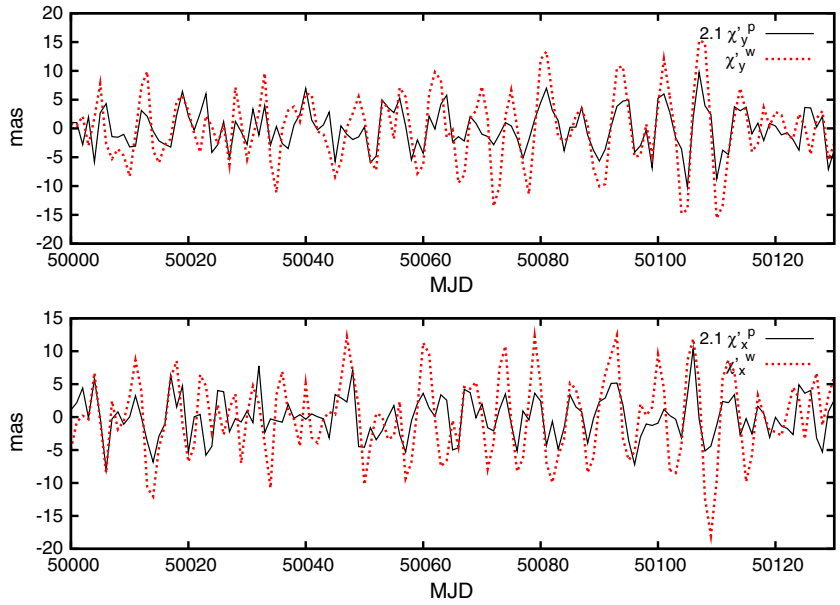

Figure 2. Equatorial components *X* and *Y* of the Celestial Atmospheric Angular Momentum for wind term χ_w and NIB pressure term χ_p multiplied by 2.1 (linear regression coefficient from 1949 to 2014) computed from NCEP AAM series after eliminating long-term periods above 1 month. Extract over 130 days, date in modified Julian day (MJD).

cpd in the TRF). The retrograde part of the spectrum only exhibits power at −365 days (ψ_1) and −182 days (Φ_1). These seasonal oscillations have been extensively analyzed by various authors, especially with regard to their observable effects on Earth's nutation [*Zharov*, 1997; *Bizouard et al.*, 1998; *Yseboodt et al.*, 2002]. We rather focus on the rapid band of the CEAM between 2 days and 30 days, of which the spectral zoom clearly unveils a harmonic at +13.6 days (25.8 h in the TRF) and a broadband peak around +7 days (28 h in the TRF). This band is isolated in time domain by using an appropriate high-band-pass filter, having an admittance of 99% at 30 days. An extract over 130 days (from modified Julian day (MJD) 50,000 to MJD 50,130) of the obtained time series is depicted in Figure 2, showing both wind terms in *X* and *Y* components as well as the full Noninverted Barometer (NIB) pressure terms that are void of any approximative correction for the oceanic response to air pressure variations. It is remarkable that for *X* and *Y* coordinates, wind and pressure terms are evidently proportional. This finding is not limited to the considered time interval, as correlations throughout the period 1949–2014 amount to 0.57 for both *X* components and *Y* components. Linear regression over the entire analysis time gives $\chi'_w \sim 2.1\chi'_p$. For the case of a hydrostatic response of the oceans (Inverted Barometer or IB approximation) imposed on the CEAM, the ratio χ'_w/χ'_p increases up to 5, whereas the correlation drops to 0.43.

The detected proportionality appears to be a feature of the short-term CEAM from 2 days to 1 month, but it does not extend to the complementary spectral bands, ranging from 1 month to several years, where correlations between pressure and wind terms drop to 0.1. Another striking feature distinguishing the 2–30 day band from other parts of the spectrum is the fact that contributions of Northern and Southern Hemispheres to the wind terms have synchronous variations with similar phases and amplitudes, as evidenced by Figure 3. Such a behavior is not observed for the S_1 thermal wave for which Southern and Northern Hemispheres contribute asymmetrically to χ'_w with a phase lag of 6 months.

All these results are confirmed by an analogous analysis of European Centre for Medium-Range Weather Forecasts (ECMWF) AMF time series as downloaded from the GeoForschungsZentrum Postdam ftp server ftp://ftp.gfz-postdam.de/pub/home/ig/ops/.

Meaning of the proportionality between pressure and wind term: Let $\vec{\Gamma}$ be the torque that the atmosphere exerts on the solid Earth. It is composed of the bulge torque $\vec{\Gamma}_b$ acting on the equatorial bulge because of pressure and gravitational forces, and of a local torque $\vec{\Gamma}_l$ caused by pressure on the local topography as well as the friction drag on Earth's surface [*de Viron et al.*, 1999; *Schindelegger et al.*, 2013]. In the nonrotating frame we have the following complex quantities: $H'_{w/p}$ for the equatorial wind/pressure term, Γ'_l for the local

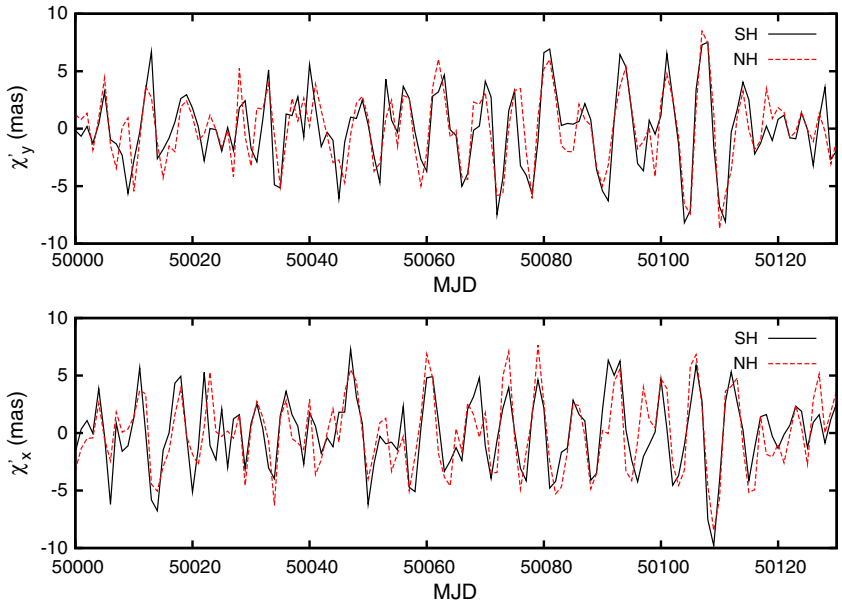

Figure 3. Contributions of the Southern Hemisphere (SH) and Northern Hemisphere (NH) to the wind term in (bottom) χ'_X and (top) χ'_Y for the 2–30 day band. Time series of 130 days, commencing at modified Julian day 50,000 (10 October 1995).

torque, Γ'_b for the bulge torque, and Γ'_{ext} for the external gravitational torque on the atmosphere. Following our derivations in Appendix A (equation (A10)), it can be established in frequency domain that

$$1 - \frac{\sigma'}{\Omega} - \frac{\sigma'}{\Omega}\frac{\hat{H}'_w}{\hat{H}'_p} = \frac{-\hat{\Gamma}'_l + \hat{\Gamma}'_{\text{ext}}}{\hat{\Gamma}'_b}\,, \tag{8}$$

where the sign "^" corresponds to the Fourier transform. If the residual torque $-\hat{\Gamma}'_l + \hat{\Gamma}'_{\text{ext}}$ is much smaller than the bulge torque Γ'_b then

$$\hat{H}'_w \approx \frac{\Omega - \sigma'}{\sigma'}\hat{H}'_p\,. \tag{9}$$

For positive angular frequencies σ' of the filtered CEAM, with periods from 2 days to 1 month, we have $1/30\,\Omega \le \sigma' \le 1/2\,\Omega$ (the retrograde part of the spectrum is much smaller); so according to (9) pressure and wind terms become almost proportional. This is in contrast with the seasonal band (S_1 in the TRF) where the smallness of the local torque with respect to the bulge torque is not satisfied [*Marcus et al.*, 2004]. Considering for the lunar tidal band a typical magnitude of $|\chi'_p| \sim 0.2$ milliseconds of arc (mas) (see spectrum of Figure 1), the bulge torque magnitude, given by $|\Gamma'_b| = \Omega|H'_p| = \Omega^2(C-A)|\chi'_p|$ [*Marcus et al.*, 2004], amounts to $\sim$1.5 10^{18} Nm. According to *Bizouard and Lambert* [2001], the external torque Γ'_{ext} is mostly composed of a 13.6 day component with an amplitude of $\sim 10^{17}$ Nm, which is at least 10 times smaller than the equatorial bulge torque $\Omega|H'_p|$. Hence, as far as the local torque does not exceed the order of magnitude of the external torque, the above condition holds.

4. Tidally Coherent Fit of the 13.6 Day Term

As emphasized by the spectral zoom of Figure 1, the main peak is at 13.66 days. The most natural hypothesis for its origin is the diurnal tidal wave O_1 determined by the Delaunay argument $2(F + \Omega)$ in the nonrotating frame, with $F = \overline{\omega} + l$ being the sum of the perigee argument $\overline{\omega}$ and the mean anomaly l, and Ω being the longitude of the ascending node of the Moon on the ecliptic plane. Note that $s = F + \Omega$ is the mean tropic longitude of the Moon.

As expected from tidal theory, the main peak is accompanied by a sidelobe at 13.63 days having the argument $2F + \Omega$. These two components differ by the frequency Ω of the displacement of the ascending node of the Moon, that is 1/18.6 cpy (cycles/year). The fact that we observe both of these peaks in CEAM substantiates the tesseral lunar influence on CEAM, in particular on the wind component.

The celestial oscillations of arguments $\Phi_1 = 2F + 2\Omega = 2s$ (13.66 days) and $\Phi_2 = 2F + \Omega$ (13.63 days) are fitted by a least squares method to the model

$$\chi' = \sum_{j=1}^{2} (m_c^j + i m_s^j) e^{i(\phi_j + \pi/2)} \,. \tag{10}$$

For the period 1949–2013 we obtain

$$\begin{aligned} \chi_p'^{\mathrm{IB}}[\mathrm{mas}] &= (0.05 - i0.02)\, e^{i(\phi_1+\pi/2)} + (0.02 - i0.00)\, e^{i(\phi_2+\pi/2)} \\ \chi_p'^{\mathrm{NIB}}[\mathrm{mas}] &= (0.17 - i0.06)\, e^{i(\phi_1+\pi/2)} + (0.06 - i0.01)\, e^{i(\phi_2+\pi/2)} \\ \chi_w'[\mathrm{mas}] &= (0.73 - i0.04)\, e^{i(\phi_1+\pi/2)} + (0.23 - i0.01)\, e^{i(\phi_2+\pi/2)} \end{aligned} \tag{11}$$

The m_s terms are small relatively to m_c, except for the IB term where about two thirds of the regional contribution of the pressure field—the oceanic one—has been replaced by a time-variable mean value computed from all pelagic points. Disregarding the IB solution, the harmonic coefficients are therefore almost in phase with the tidal wave of argument $\phi_i + \pi/2$, confirming the proportionality of wind and pressure terms at this period and supporting their common tidal gravitational cause. The ratio $\chi_w'/\chi_p'^{\mathrm{NIB}} = H_w'/H_p' \sim 4$ for both tidal frequencies does not match the numerical value of the condition (9), namely, $H_w'/H_p' = 13.6 - 1 \sim 13$. To explain this difference, it does seem unreasonable to assume that the wind term is underestimated, e.g., as a consequence of the 10 mbar vertical boundary of the NCEP/NCAR model that neglects only about 1% of the total atmospheric mass. On the other hand, the ratio $\chi_w'/\chi_p'^{\mathrm{IB}} \approx 14$ much better fits the expected ratio of 12.6, as if the effective pressure term around the O_1 frequency was the one restricted to continents and a static IB ocean. This is quite peculiar, since an IB response of the oceans is generally observed above 10 days but not at diurnal periods in the TRF [*Salstein and Rosen*, 1989].

Moreover, at the O_1 frequency the fit is consistent with the external gravitational torque in the true equatorial frame [*Bizouard and Lambert*, 2001]. Indeed, this quantity reads

$$\Gamma_{\mathrm{ext}}'(O_1) \approx -0.8\, 10^{17}[\mathrm{N\,m}] e^{i\phi_1} \tag{12}$$

and is in quadrature of phase with respect to the corresponding harmonics of the wind and IB pressure terms of expression (11).

Temporal variability: By reference to the high-frequency CEAM model

$$\chi' = \sum_{j=1}^{2} \left(m_c^j + i\, m_s^j\right)\, e^{i(\phi_j(t)+\pi/2)}$$

with $\phi_1 = 2(F + \Omega)$ (13.66 days, O_1 tidal wave in the TRF) and $\phi_2 = \phi_1 + 2l_m$ (l_m is the mean anomaly of the Moon) representing the weekly signal (6.86 days, 2Q1 tidal wave in the TRF), the parameters m_c and m_s were adjusted repeatedly in a sliding window of 6 years. The results are reported in Figure 4 for pressure and wind terms. The IB pressure term at 13.6 days, and the NIB pressure term at 6.8 days are multiplied by the corresponding theoretical ratio from (9) for χ'^w/χ_p'. For these harmonics, the coherency in the variations of χ_p' and χ_w' are overwhelming. We notice an 18–20 year modulation for the 13.66 day term, reflecting the beating produced by the 13.63 day term.

5. The Quasi-Weekly Band

As shown by the Gabor decomposition in Figure 5, the broadband peak between 5 and 8 days is much more powerful than the thin peaks around 13.6 days, showing episodes with an amplitude of 10 mas. Some studies like *Brzeziński et al.* [2002] attribute this weekly signal to the retrograde Rossby-Haurwitz atmospheric normal mode Ψ_1^1, having in the TRF the geometry of a spherical harmonic $\cos(\phi)e^{i\lambda}$ (ϕ is the latitude, λ is the longitude) propagating to the west [*Volland*, 1996]. On the other hand, in the nonrotating frame, this resonant mode propagates from the west to the east as the Moon, and with an averaged period of ~7 days it could be amplified at planetary scale by the minor lunar tides $2Q_1$ (6.86 days) and σ_1 (7.09 days) (at least 100 times smaller than O_1). As shown by the associated sliding window least squares fit plotted in Figure 4, the linear correlation between variable parts of the wind and NIB pressure term is even more striking than at 13.6 days (above 0.7). Moreover, at quasi-weekly periods ($\sigma'/\Omega \approx 1/7$) the ratio $\chi_w'/\chi_p'^{\mathrm{NIB}} \approx 5.8$ fits the

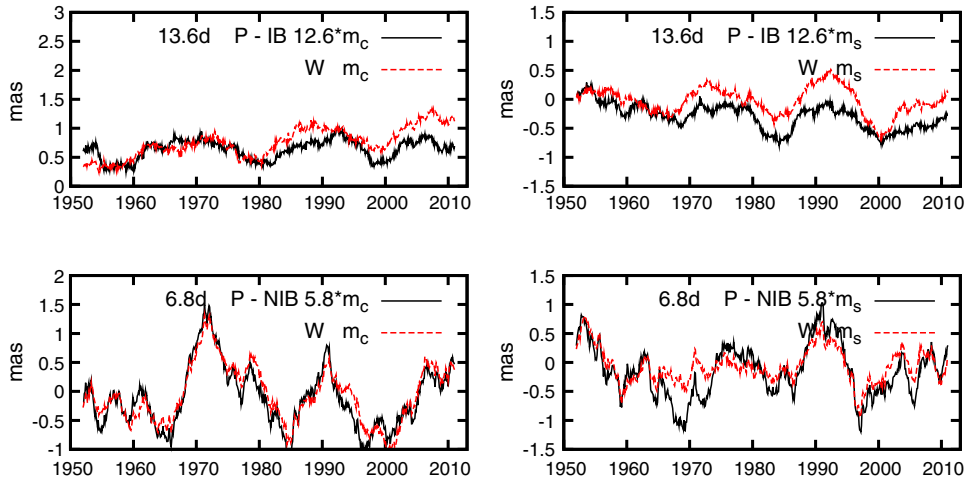

Figure 4. Variability of 13.66 day and 6.8 day components of the winds and pressure terms. Six year sliding window fit of (left column) m_c and (right column) m_s parameters in the model $(m_c + im_s)\,e^{i\Phi}$, where Φ is the tidal argument. The NIB or IB pressure terms are multiplied by the theoretical ratio (9) corresponding to the considered period.

condition (9) reading $H'_w/H'_p \approx 7 - 1 = 6$ and is thus valid for the full pressure term in contrast to what is observed at 13.6 days. Our validation against complementary series from the ECMWF model reproduced quite well the results associated with NCEP data over the period 1985–2013, except for the wind component at 13.6 days, which contained a relatively large out-of-phase term m_s (0.5 instead of 0.07 mas).

6. Hydrostatic Model of the Tidal O_1 Oscillation of the Pressure Term

Why is the phase of the O_1 oscillation of the CEAM precisely $\Phi_1 = 2(F + \Omega) + \pi/2$? Let us investigate this question by assuming a simple hydrostatic redistribution of the air masses under the action of the lunar tidal force. Because of the lunar tidal potential U_1, surface pressure undergoes a variation from P_0 to $P_0 + P_1$, satisfying

$$\vec{\nabla}P_0 + \vec{\nabla}P_1 = -(\rho_0 + \rho_1)\vec{\nabla}(U_0 + U_1) \tag{13}$$

where U_0 is the nonperturbed geopotential, $\rho_0 \approx 1.3$ kg/m^3 is the nonperturbed uniform air density and ρ_1 denotes the variation of the air density caused by the tide. Assuming that there is no tidally induced circulation at Earth's surface (references are given at the end of this section), the air density ρ_0 is constant at any place according to the continuity equation, and $\rho_1 \approx 0$. After neglecting second-order terms in (13), and accounting for hydrostatic equilibrium $\vec{\nabla}P_0 = -\rho_0\vec{\nabla}U_0$ in the nonperturbed state, we obtain by omission of the gradient of ρ_0

$$\vec{\nabla}P_1 = -\vec{\nabla}(\rho_0 U_1)\,. \tag{14}$$

In turn we have

$$P_1 = -\rho_0 U_1\,. \tag{15}$$

According to classic tidal theory [*Sidorenkov*, 2009; *Simon et al.*, 2013], at the Earth surface the tesseral daily tide caused by the Moon is expressed by

$$U_1 \approx 2G_M\,[1 + m\cos(s - p)]\;\sin 2\phi\,\sin\varepsilon\,\sin s\cos H\,, \tag{16}$$

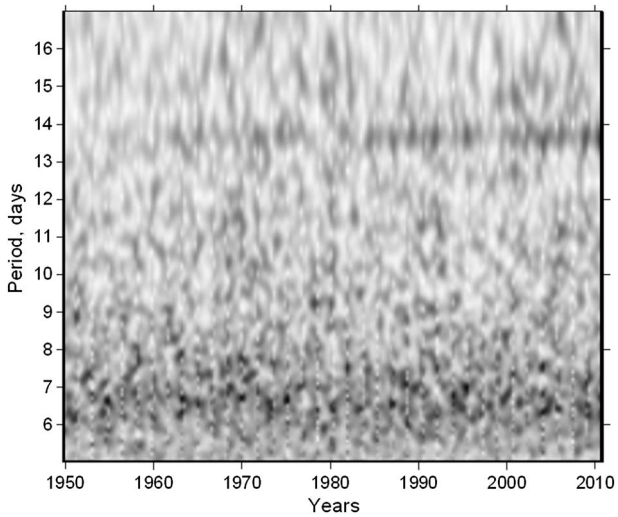

Figure 5. Gabor decomposition of the CEAM—wind term from 1950 to 2010 in the lunar tidal band 2–20 days.

where $G_M = 2.64\ \mathrm{m}^2/\mathrm{s}^2$ is the Doodson constant for the Moon; s is the mean tropic longitude of the Moon, $s = F + \Omega$, already introduced; p is the mean tropic longitude of the Moon perigee; $m = 0.165$ is the amplitude modulation associated with the elliptical orbit of the Moon; ϕ is the latitude; $\varepsilon = 23.7°$ is the obliquity of the ecliptic; and H is the hour angle of the Moon.

It is straightforward to show that

$$U_1 \approx G_M\,[1 + m\cos(s-p)]\sin 2\phi \sin\varepsilon(\sin(s-H) + \sin(s+H))\ . \tag{17}$$

The main terms are those directly proportional to $\sin(s+H)$ corresponding to the K_1 tide (constant term in the nonrotating frame), and to $\sin(s-H)$, corresponding to the O_1 tide, and have the same amplitude. In fact, the K_1 peak in AAM mostly results from annual modulation of the thermal diurnal cycle S_1 [*Bizouard et al.*, 1998], and the tidal contribution represents a small fraction of this spectral component. We focus on the O_1 tesseral potential

$$U_1(O_1) \approx G_M \sin 2\phi \sin\varepsilon \sin(s-H)\ . \tag{18}$$

As $s = \mathrm{GST} + \lambda - H$, where λ is the longitude of the place under consideration, we have $-H = -\mathrm{GST} - \lambda + s$ and

$$\begin{aligned} U_1(O_1) &= \frac{2}{3} G_M P_2^1(\cos\phi)\sin\varepsilon \sin(2s - \mathrm{GST} - \lambda) \\ &= \frac{2}{3} G_M P_2^1(\cos\phi)\sin\varepsilon\,(\sin(2s-\mathrm{GST})\cos\lambda - \cos(2s-\mathrm{GST})\,,\sin\lambda)\ , \end{aligned} \tag{19}$$

where $P_2^1(\cos\phi) = 3\cos\phi\sin\phi$ is the second-order tesseral Legendre polynomial. So according to (15)

$$P_1 = (p_{21}\cos\lambda + \tilde{p}_{21}\sin\lambda)P_2^1(\cos\phi) \tag{20}$$

with $p_{21} = -\rho_0 \frac{2}{3} G_M \sin\varepsilon \sin(2s - \mathrm{GST})$, $\tilde{p}_{21} = \rho_0 \frac{2}{3} G_M \sin\varepsilon \cos(2s - GST)$. However, according to equation (B3) (Appendix B), the AAM pressure term can be directly derived from the tesseral component of the surface pressure

$$\chi_p \approx -\frac{4\pi}{5}\frac{r_0^4}{(C-A)g}(p_{21} + i\tilde{p}_{21})\ , \tag{21}$$

where $r_0 \approx 6371$ km is the mean equatorial radius of the Earth and $g \approx 9.81\mathrm{m/s}^2$ represents the mean gravity acceleration in the vicinity of Earth's surface. So the pressure term variation engendered by the Moon is

$$\begin{aligned} \chi_p &\approx -\frac{4\pi}{5}\frac{r_0^4}{(C-A)g}\rho_0\frac{2}{3}G_M \sin\varepsilon\,(-\sin(2s-\mathrm{GST}) + i\cos(2s-\mathrm{GST})) \\ &\approx -\frac{8\pi}{15}\frac{r_0^4}{(C-A)g}\rho_0 G_M i \sin\varepsilon\ e^{i(2s-\mathrm{GST})}\ , \end{aligned} \tag{22}$$

and the corresponding CEAM reads

$$\chi_p' = -\chi_p e^{i\mathrm{GST}} \approx \frac{8\pi}{15}\frac{r_0^4}{(C-A)g}\rho_0 G_M \sin\varepsilon\ e^{i(2s+\pi/2)}\ , \tag{23}$$

not only accounting for the order of magnitude of the actually observed O_1 pressure term in (11) (0.2 mas) but also reproducing its phase.

Can we also explain the amplitude and the phase of the O_1 wind term? If the hydrostatic assumption is true for surface pressure, tidal winds do not blow at Earth's surface, but at high altitudes. Tidal lunar variation of the horizontal wind have been indeed reported in the mesosphere (above 50 km) [*Sandford et al.*, 2006], in the stratosphere [*Nastrom and Belmont*, 1976; *Sakazaki et al.*, 2010], in the upper troposphere [*Krahenbuhl et al.*, 2011], but never in the low troposphere. So tidal winds do not produce any notable friction torque. On the other hand, a tesseral tidal pressure field exerts a torque on the bulge but cannot contribute to the topographic torque, which results from spherical harmonics of degree higher than 3 [*Dehant et al.*, 1996]. We thus conclude that the tidal atmospheric circulation does not contribute significantly to the local torque, in accordance with condition (9) and that it accounts for the proportionality of χ_w' and χ_p'. As noted earlier, we obtain the expected ratio for 7 day oscillations, but for 13.6 days the theoretical constraint is satisfied only if we resort to the IB pressure term and not to the total matter term of the atmospheric angular momentum.

7. Effect on Earth's Nutation

The action of the lunisolar tesseral forces on the equatorial bulge yields prograde terms of the nutation below 30 days, with amplitudes of up to 100 mas (13.6 day component). These terms are modeled precisely by taking into account Earth's nonrigidity and the ocean tides. However, the celestial pole offsets, i.e., the corrections to the IERS conventional nutation model, as obtained from the processing of VLBI (Very Long Baseline Interferometry) observations, have still a standard deviation of about 100 μas in the 5–15 day band, thereby revealing deficiencies of the model. The latter could result from the atmospheric lunar tide. Considering the effective CEAM $\chi_e'^p = 1.01\chi'^p$ and $\chi_e'^w = 1.6\chi'^w$, the nutation effect can be estimated from the frequency transfer function of *Sasao and Wahr* [1981] or *Brzeziński* [1994, equation (4.9)]:

$$P(\sigma') = T_p(\sigma')\chi_e'^p(\sigma') + T_w(\sigma')\chi_e'^w(\sigma'), \tag{24}$$

in which

$$T_p(\sigma') = \sigma_c \left[\frac{1}{\sigma_c' - \sigma'} + \frac{a_p}{\sigma_f' - \sigma'} \right], \tag{25}$$

and a similar expression can be phrased for T_w using the coefficient a_w. Here T_p and T_w are transfer functions of the pressure term and of the wind term, respectively, σ' is the nutation angular frequency, $\sigma_c' = \sigma_c + \Omega$ and $\sigma_f' \approx -\Omega/430\,(1 - i/40,000)$ are the space-referred angular frequencies of the Chandler wobble and of the Free Core Nutation (FCN) modes, $\sigma_c \approx \Omega/433\,(1 + i/200)$ is the Earth-referred Chandler frequency, and $a_p = 9.509 \times 10^{-2}$, $a_w = 5.489 \times 10^{-4}$ are dimensionless coefficients expressing the response of the FCN mode to pressure and wind excitations [*Brzeziński*, 1994].

Using the above expression, it can be estimated that for prograde circular excitations of periods spanning from 2 days to 1 month, $T_w(\sigma')$ is at least 2 times larger than $T_p(\sigma')$, with T_w presenting a rather constant value: $T_w(\Omega/7) \sim 2.6\,10^{-3}$ and $T_w(\Omega/13.6) \sim 2.3\,10^{-3}$. Given that the pressure term is about 5 times smaller than the wind term, its effect can be neglected. With amplitudes in χ_w' reaching 10 mas, broadband oscillation of the wind term around 7 days can produce a nutation of about $10 \times 2.6\,10^{-3} \sim 0.03$ mas; cf. estimates of *Schindelegger et al.* [2011]. Until now, these periodicities are poorly covered by space geodetic techniques, since nutation is routinely monitored by aid of VLBI observations with a mean temporal resolution of about 7 days. However, various attempts to densify nutation determination by jointly processing GNSS (Global Navigation Satellite System) data seem to confirm this broadband nutation with the estimated order of magnitude [*Bizouard et al.*, 2010]. The tidal atmospheric effect on the 13.6 day nutation has an average magnitude of $1 \times 2.3\,10^{-3} = 0.003$ mas. The 13.6 day term fit in celestial pole offset time series depends on the series produced by the various analysis centers of the International VLBI Service, with amplitude discrepancies ranging from 5 to 15 μas, and phase offsets of up to 180° (on the website of the IERS Earth Orientation Center, http://hpiers.obspm.fr, this fit can be performed with eight available VLBI series). Considering the smallness of the corresponding atmospheric effect, it is not possible to make any sound conclusion about its observability in nutation.

8. Conclusion

Below periods of 1 month, the Celestial Equatorial Atmospheric Angular Momentum is mostly composed of prograde oscillations, dominated by a harmonic at 13.6 days and a broadband peak around 7 days, initially detected in the terrestrial frame [*Brzeziński et al.*, 2002]. The present study aimed at showing that this band has a lunar tidal origin, suggested by two specific features that contrast with what is observed for seasonal CEAM variations of thermal origin: (i) Northern and Southern Hemispheres contribute equally and synchronously to the globally integrated signal and (ii) pressure and wind terms are almost proportional to each other.

The 13.6 day pressure term clearly results from the main lunar tide, explained by a hydrostatic reaction to the tesseral O_1 tidal forcing. The origin of the broadband peak around 7 days in the nonrotating frame is less evident. The weekly variation possibly results from the lunar tide, of which the effect is amplified by the Ψ_1^1 atmospheric resonance.

As the surface pressure response to the lunar tesseral potential seems to be hydrostatic, the tidal flow is only significant at high altitudes, and the topographic and friction torques are negligible compared to the

bulge torque for periods between 2 days and 1 month in the nonrotating celestial frame. This constellation accounts for the proportionality between pressure and wind terms. While around 7 days (28 h in the TRF) the observed ratio fits the theoretical ratio for the full (NIB) pressure term, at the tidal period of 13.6 days (25.8 h in the TRF) the theoretical ratio oddly matches the case of the IB pressure term, as if the oceans and the atmosphere were hydrostatically coupled.

Our quintessential conclusion is as follows: from 24.8 h to 48 h in the TRF the retrograde equatorial atmospheric angular momentum variations are mostly triggered by the Moon. In order to observe a possible effect on nutation, improvements of the VLBI/GNSS data processing as well as optimized observation schedules are required. Characterization of the regional atmospheric contributions is likely to yield further insights into the associated mass transport mechanism.

Appendix A: Relation Between Atmospheric Torques and Angular Momentum in Nonrotating Frame

Let $\vec{\Gamma}$ be the torque that the atmosphere exerts on the solid Earth. It is composed of the bulge torque $\vec{\Gamma}_b$ acting on the equatorial bulge because of the pressure and gravitational forces, and of a local torque $\vec{\Gamma}_l$ caused by pressure on the topography and friction drag at Earth's surface. Let H_p be the equatorial pressure term of AAM and recall that [*Marcus et al.*, 2004]

$$\Gamma_b = -i\Omega H_p \,, \tag{A1}$$

where Γ_b is the complex equatorial component of $\vec{\Gamma}_b$ in the TRF. The angular momentum balance of the atmosphere states that

$$\frac{\mathrm{d}\vec{H}}{\mathrm{d}t} = -\vec{\Gamma}_b - \vec{\Gamma}_l + \vec{\Gamma}_{\mathrm{ext}} \tag{A2}$$

where $\vec{H}$ is the total atmospheric angular momentum and $\vec{\Gamma}_{\mathrm{ext}}$ is the lunisolar torque on the atmosphere, of which the estimation can be found in *Bizouard and Lambert* [2001]. Let H_w be the equatorial complex component of the wind term. Written in the TRF, the former equation allows us to establish that

$$\dot{H}_p + \dot{H}_w + i\Omega(H_p + H_w) = -\Gamma_b - \Gamma_l + \Gamma_{\mathrm{ext}} \,, \tag{A3}$$

where Γ_l and Γ_{ext} are the components of $\vec{\Gamma}_l\, \vec{\Gamma}_{\mathrm{ext}}$ in the TRF, respectively. Considering (A1), we can eliminate Γ_b and obtain

$$\dot{H}_p + \dot{H}_w + i\Omega H_w = -\Gamma_l + \Gamma_{\mathrm{ext}} \,. \tag{A4}$$

This equation is transferred in the true equatorial frame by multiplying both sides by $e^{i\theta}$:

$$(\dot{H}_p + \dot{H}_w)e^{i\theta} + i\Omega H'_w = -\Gamma'_l + \Gamma'_{\mathrm{ext}} \,, \tag{A5}$$

where Γ'_l and Γ'_{ext} represent the complex equatorial components of the corresponding torques and H'_w is the celestial wind term. Equivalently, we have

$$\frac{\mathrm{d}\left(H_p e^{i\theta} + H_w e^{i\theta}\right)}{\mathrm{d}t} - i\dot{\theta}(H_p + H_w)e^{i\theta} + i\Omega H'_w = -\Gamma'_l + \Gamma'_{\mathrm{ext}} \,. \tag{A6}$$

As $\dot{\theta} = \Omega$, the former equation becomes

$$\dot{H'}_p + \dot{H'}_w - i\Omega(H'_p + H'_w) + i\Omega H'_w = -\Gamma'_l + \Gamma'_{\mathrm{ext}} \tag{A7}$$

or

$$\dot{H'}_p + \dot{H'}_w - i\Omega H'_p = -\Gamma'_l + \Gamma'_{\mathrm{ext}} \,. \tag{A8}$$

Applying the Fourier transform (denoted by the symbol ˆ) with the celestial angular frequency $\sigma' \ll \Omega$ yields

$$i(\sigma' - \Omega)\hat{H}'_p + i\sigma'\hat{H}'_w = -\hat{\Gamma}'_l + \hat{\Gamma}'_{\mathrm{ext}} \,. \tag{A9}$$

Then, by dividing by $\hat{\Gamma}'_b = -i\Omega\hat{H}'_p$ deduced from (A1), we obtain an equation similar to equation (11) of *Marcus et al.* [2004] expressed in the TRF but including now the external gravitational torque

$$1 - \frac{\sigma'}{\Omega} - \frac{\sigma'}{\Omega}\frac{\hat{H}'_w}{\hat{H}'_p} = \frac{-\hat{\Gamma}'_l + \hat{\Gamma}'_{\mathrm{ext}}}{\hat{\Gamma}'_b} \,. \tag{A10}$$

Appendix B: Pressure Term Reduced to the Tesseral Pressure Field

The pressure term can be expressed by [*Bizouard*, 2014]

$$\chi^p = -\frac{r_0^4}{3N_2^1(C-A)g}\int_{\theta=0}^{\pi}\int_{\lambda=0}^{2\pi} P_s Y_2^1 \sin\theta \, d\theta \, d\lambda \tag{B1}$$

where λ is the longitude, θ the colatitude, r_0 the mean Earth radius, g the mean surface gravity acceleration, P_s the surface pressure, and Y_2^1 the complex spherical harmonic function $P_2^1(\sin\theta)e^{i\lambda}$ normalized by $N_2^1 = \sqrt{(5/24\pi)}$. The surface pressure is developed in complex spherical harmonics

$$P_s = \sum_{l=0}\sum_{m=-l}^{l} p'_{lm} Y_l^m(\theta,\lambda) \tag{B2a}$$

with

$$p'_{lm} = \frac{p_{lm} - i\tilde{p}_{lm}}{2N_l^{|m|}} \text{for } m>0 \quad , \quad p'_{l0} = \frac{p_{l0}}{N_l^0} \quad , \quad p'_{lm} = \frac{p_{lm} + i\tilde{p}_{lm}}{2N_l^{|m|}} \text{for } m<0\,. \tag{B2b}$$

Inserting this development of P_s in (B1) and taking into account orthonormality relations between Y_2^1 and the other Y_l^m, we obtain

$$\chi^p = -\frac{r_0^4}{3N_2^1(C-A)g}p'_{2,-1} = -\frac{4\pi}{5}\frac{r_0^4}{(C-A)g}(p_{21} + i\tilde{p}_{21})\,, \tag{B3}$$

which is reduced to the tesseral component (2, 1) of the pressure field.

Acknowledgments
We are grateful to the Paris Observatory for allocating a 2 month position to Leonid Zotov. This greatly helped us to carry out this work. We are indebted to Michael Schindelegger of TU Vienna for improving the quality of this paper. The atmospheric angular momentum data (NCEP/NCAR reanalyses) associated with the results shown in this paper were prepared by the Special Bureau for Atmosphere within the IERS Global Geophysical Fluids Center (downloaded from http://ftp.aer.com/pub/anon_collaborations/sba/).

References

Barnes, R. T. H., R. Hide, A. A. White, and C. A. Wilson (1983), Atmospheric angular momentum fluctuations, length-of-day changes and polar motion, *Proc. R. Soc. A*, *387*, 31–73.
Bizouard, C. (2014), *Le Mouvement du Pôle de L'Heure au Siècle*, 284 pp., Presses Académiques Francophones. [Available at www.presses-academiques.com.]
Bizouard, C., and S. Lambert (2001), Lunisolar torque on the atmosphere and Earth's rotation, *Planet. Space Sci.*, *50*(3), 323–333.
Bizouard, C., and L. Seoane (2010), Atmospheric and oceanic forcing of the rapid polar motion, *J. Geodesy*, *84*, 19–30, doi:10.1007/s00190-009-0341-2.
Bizouard, C., A. Brzeziński, and S. Petrov (1998), Diurnal atmospheric forcing and temporal variations of the nutation amplitudes, *J. Geodesy*, *72*, 561–577.
Bizouard, C., J. Y. Richard, S. Bolotin, and O. Bolotina (2010), High frequency nutation from GRGS multitechnique combination, paper presented at 6th Orlov Conference, Kiev, July 2009.
Brzeziński, A. (1994), Polar motion excitation by variations of the effective angular momentum function. II: Extended model, *Manuscr. Geod.*, *19*, 157–171.
Brzeziński, A., C. Bizouard, and S. Petrov (2002), Influence of the atmosphere on Earth rotation: What new can be learnt from the recent atmospheric angular momentum estimates?, *Surv. Geophys.*, *23*, 33–69.
Chapman, S., and R. Lindzen (1970), *Atmospheric Tides: Thermal and Gravitational*, D. Reidel Publishing Company, Dordrecht, Holland.
Dehant, V., C. Bizouard, J. Hinderer, H. Legros, and M. Leffzt (1996), On atmospheric pressure perturbations on precession and nutations, *Phys. Earth Planet Inter.*, *96*, 25–39.
de Viron, O., C. Bizouard, D. Salstein, and V. Dehant (1999), Atmospheric torque on the Earth and comparison with atmospheric angular momentum variations, *J. Geophys. Res.*, *4861–4875*(B3).
IERS Conventions (2010), *IERS Technical Note 36*, G. Petit and B. Luzum (ed.), 179 pp., Verlag des Bundesamts fuer Kartographie und Geodäsie, Frankfurt am Main. [Available at http://tai.bipm.org/iers/conv2010/conv2010.html.]
Krahenbuhl, D. S., M. B. Pace, R. S. Cerveny, and R. C. Balling Jr. (2011), Monthly lunar declination extremes influence on tropospheric circulation patterns, *J. Geophys. Res.*, *116*, D23121, doi:10.1029/2011JD016598.
Li, G. (2005), 27.3-day and 13.6-day atmospheric tide and lunar forcing on atmospheric circulation, *Adv. Atmos. Sci.*, *22*(3), 359–374.
Li, G., H. Zong, and Q. Zhang (2011), 27.3-day and average 13.6-day periodic oscillations in the Earth's rotation rate and atmospheric pressure fields due to celestial gravitation forcing, *Adv. Atmos. Sci.*, *28*(1), 45–58.
Marcus, S., O. de Viron, and J. Dickey (2004), Atmospheric contributions to Earth Nutation: Geodetic constraints and limitations of the torque approach, *J. Atmos. Sci.*, *61*, 352–356.
Nastrom, G. D., and A. D. Belmont (1976), Diurnal stratospheric tide in meridional wind, 30 to 60 km by season, *J. Atmos. Sci.*, *33*, 315–320.
Sakazaki, T., M. Fujiwara, and H. Hashiguchi (2010), Diurnal variations of upper tropospheric and lower stratospheric winds over Japan as revealed with middle and upper atmosphere radar (34.85°N, 136.10°E) and five reanalysis data sets, *J. Geophys. Res.*, *115*, D24104, doi:10.1029/2010JD014550.
Salstein, D., and R. Rosen (1989), Regional contributions to the atmospheric excitation of rapid polar motions, *J. Geophys. Res.*, *94*(D7), 9971–9978.
Sandford, D. J., H. G. Muller, and N. J. Mitchell (2006), Observations of lunar tides in the mesosphere and lower thermosphere at Arctic and middle latitudes, *Atmos. Chem. Phys.*, *6*(12), 4117–4127.
Sasao, T., and J. Wahr (1981), An excitation mechanism for the free "core nutation", *Geophys. J. R. Astron. Soc.*, *64*, 729–746.

SBA (2014), *Website of the IERS Special Bureau for the Atmosphere*. [Available at http://geophy.uni.lu/ggfc-atmosphere.html. Accessed date: October 2014.]
Schindelegger, M., J. Böhm, D. Salstein, and H. Schuh (2011), High-resolution atmospheric angular momentum functions related to Earth rotation parameters during CONT08, *J. Geod.*, *85*(7), 425–433.
Schindelegger, M., D. Salstein, and J. Böhm (2013), Recent estimates of Earth-atmosphere interaction torques and their use in studying polar motion variability, *J. Geophys. Res. Solid Earth*, *118*, 4586–4598, doi:10.1002/jgrb.50322.
Sidorenkov, N. S. (2009), *The Interaction Between Earth's Rotation and Geophysical Processes*, 305 pp., Wiley-VCH, Weinheim, Germany.
Sidorenkov, N. S. (2010a), Luni-solar tides in the Earth's atmosphere, paper presented at 6th Orlov Conference, Kiev, July 2009.
Sidorenkov, N. S. (2010b), *About Inaccurate Estimation of the Role of Tidal Phenomena in Geophysics*, vol. 11, special issue: 119–128, Geophys. Res., Russian Acad. Sc., in Russian.
Simon, B., A. Lematre, and J. Souchay (2013), Oceanic tides, in *Lecture Note in Physics*, vol. 861, pp. 83–114, Springer, Berlin Heidelberg.
Volland, H. (1996), Atmosphere and Earth's rotation, *Surv. Geophys.*, *17*(1), 101–144.
Yseboodt, M., O. de Viron, T. M. Chin, and V. Dehant (2002), Atmospheric excitation of the Earth's nutation: Comparison of different atmospheric models, *J. Geophys. Res.*, *107*(B2), 2036, doi:10.1029/2000JB000042.
Zharov, V. E. (1997), *Sol. Syst. Res.*, *31*(6), 501.